





RESEARCH ARTICLE | AUGUST 09 2023

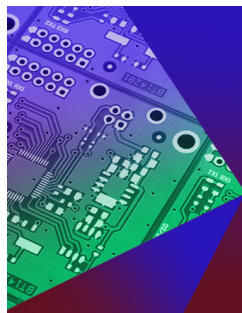
Design of vacuum system for NCST spherical tokamak

Fu Hua Huang; Dong Hua Xiao; Xiao Chang Chen ; Hui Chen ; San Qiu Liu  



AIP Advances 13, 085313 (2023)

<https://doi.org/10.1063/5.0160942>



APL Electronic Devices

Fostering connections across multiple disciplines in the broad electronics community

Follow us on  @aplecddevices



[Learn More](#)

Design of vacuum system for NCST spherical tokamak

Cite as: AIP Advances 13, 085313 (2023); doi: 10.1063/5.0160942

Submitted: 6 June 2023 • Accepted: 22 July 2023 •

Published Online: 9 August 2023



View Online



Export Citation



CrossMark

Fu Hua Huang,^{1,2} Dong Hua Xiao,^{1,2} Xiao Chang Chen,^{1,2,a)} Hui Chen,^{1,2}  and San Qiu Liu^{1,2,a)} 

AFFILIATIONS

¹Department of Physics, Nanchang University, Nanchang 330047, China

²Jiangxi Province Key Laboratory of Fusion and Information Control, Nanchang 330031, China

^{a)}Authors to whom correspondence should be addressed: xcchen1985@ncu.edu.cn and sqlgroup@ncu.edu.cn

ABSTRACT

The NanChang Spherical Tokamak (NCST) is a new compact tokamak with an aspect ratio of $R/a = 1.67$. The vacuum system is one of the most important sub-systems of the tokamak device and has been designed especially for the NCST device. It consists of three main parts: a pumping system, a gas puffing system, and a wall conditioning system. The pumping system includes two turbo-molecular pumps, a cryopump, and two rotary pumps. The gas puffing system consists of a gas supply, transfer lines, a gas reservoir, pressure gauges, and piezoelectric valves. The wall conditioning system includes baking and glow discharge cleaning functions. The vacuum system and related experimental results are described in detail in this paper. The test results indicate that the NCST vacuum system is reliable. Inside the vessel, the ultimate pressure reached 4.2×10^{-6} Pa after 307 h of pumping. The upgraded gas puffing system can accurately control the gas entering the vacuum vessel. The wall conditioning systems, such as those for baking and glow discharge cleaning, also play a very important role in plasma operation. The plasma discharge results show that the basic function of the vacuum system meets the essential requirements of the present experiments on the NCST tokamak.

© 2023 Author(s). All article content, except where otherwise noted, is licensed under a Creative Commons Attribution (CC BY) license (<http://creativecommons.org/licenses/by/4.0/>). <https://doi.org/10.1063/5.0160942>

I. INTRODUCTION

The vacuum system is an important subsystem of a tokamak and critical to the plasma discharge.¹ It includes a vacuum vessel (VV), pumping system, fueling system, and wall conditioning system.^{2,3} As an ultrahigh vacuum pressure vessel, the VV is the core component of the tokamak device and provides a high-quality vacuum environment for the plasma discharge.⁴ The function of the pumping system is to pump out the impure gases, mainly H₂O and hydrocarbon, produced during the glow discharge cleaning as well as the working gas after discharges. It also controls the particle flow in the plasma.⁵ The role of the fueling system is to send the right amount of working gas at the right time. Gas puffing (GP), super-sonic molecular beam injection (SMBI), and pellet injection (PI) are the most commonly used fueling methods.⁶ After the pumping system has been in operation for a while, the VV needs wall conditioning to further reduce the vacuum pressure. This is because when the VV reaches a high vacuum degree, the main factor affecting the vacuum degree is not the residual gas in the VV but the impurity

particles released from the VV wall. Impurity particles can be desorbed from the VV wall by baking and discharge cleaning and then removing them via the pumping system.^{7,8}

The NCST is a compact tokamak designed to explore methods of merging compression for plasma start-ups.^{9–11} It has a major radius of $R = 0.4$ m, a minor radius of $a = 0.24$ m, and a toroidal field (TF) of $B_T = 0.36$ T. The NCST is designed to obtain a plasma current of 100 kA with a discharge time of 100 ms. The assembly of the device was completed in November 2020, and the first plasma discharge was successfully achieved in July 2022. The purpose of this paper is to introduce the vacuum system of the NCST in detail.

This paper is organized as follows: The design and layout of the VV and pumping stations are described in Sec. II. Section III presents the gas puffing scheme and the measuring equipment. Section IV describes the baking and glow discharge cleaning processes. The experimental results for the vacuum system are provided in Sec. V. Finally, the summary and prospects are provided in Sec. VI.

II. VACUUM VESSEL AND PUMPING SYSTEM

The NCST VV is made of 316 L stainless steel, and its polar profile is octagonal, as shown in Fig. 1. The thickness of the steel plate in the central column is 3 mm, as marked with red lines; the rest is 6 mm thick, as marked with orange lines. The surface area of the VV is about 10.3 m^2 and the volume is about 2.5 m^3 . The VV not only provides a vacuum environment for plasma operations but also provides windows for diagnostics, fueling, and related experiments. At present, there are four ConFlat flanges (CF) with 100 mm

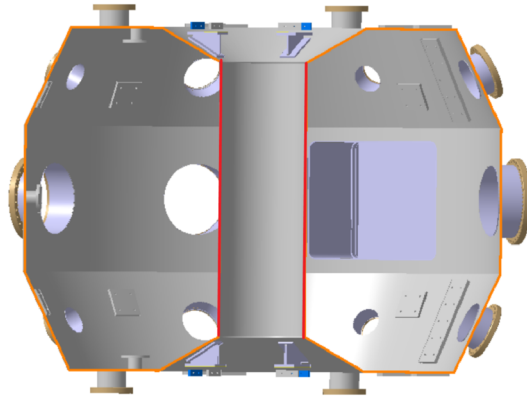


FIG. 1. Cross-section of the NCST VV.

windows installed on both the top and bottom of the VV, as well as four CF 100 mm and four CF 160 mm windows, respectively, positioned in the upper and lower sections. Additionally, there are seven CF 250 mm windows and one $500 \times 600 \text{ mm}^2$ window located in the middle section, resulting in a total of 32 windows. Generally, the tokamak VV is designed to meet the following criteria: (1) minimization of the induced eddy current in the vessel due to rapid changes in the coil currents; (2) mechanical integrity against transient loads and static loads due to the difference in pressure between the vacuum and the outside pressure; and (3) a good vacuum level for high plasma performance.¹² In order to reduce the eddy current, the thickness of the steel plate in the central column is 3 mm, thinner than that of the other steel plates. The VV structures of CFETR, HL-2M, and other large tokamaks are D-shaped because a D-shaped structure can better fit the plasma shape and is more stable than a polygonal structure.^{4,13} The NCST VV, however, has an octagonal structure. As the size and discharge parameters of the NCST are small, the stability required for the VV is reduced, and the octagonal structure can meet NCST experimental requirements while being more economical.

To meet the experimental requirements of the vacuum environment, two turbo-molecular pumps with pumping speeds of 2000 l/s are used as the main pumping devices, and two rotary pumps act as the roughing pumps, as shown in Fig. 2. The port of the NCST tokamak limits the size of the pumping duct and the choice of turbo-molecular pump. Therefore, three horizontal ports with diameters of 250 mm are selected to connect the pumping ducts. Finally, in order to pump out H_2O , N_2 , and CO_2 effectively, a cryopump with

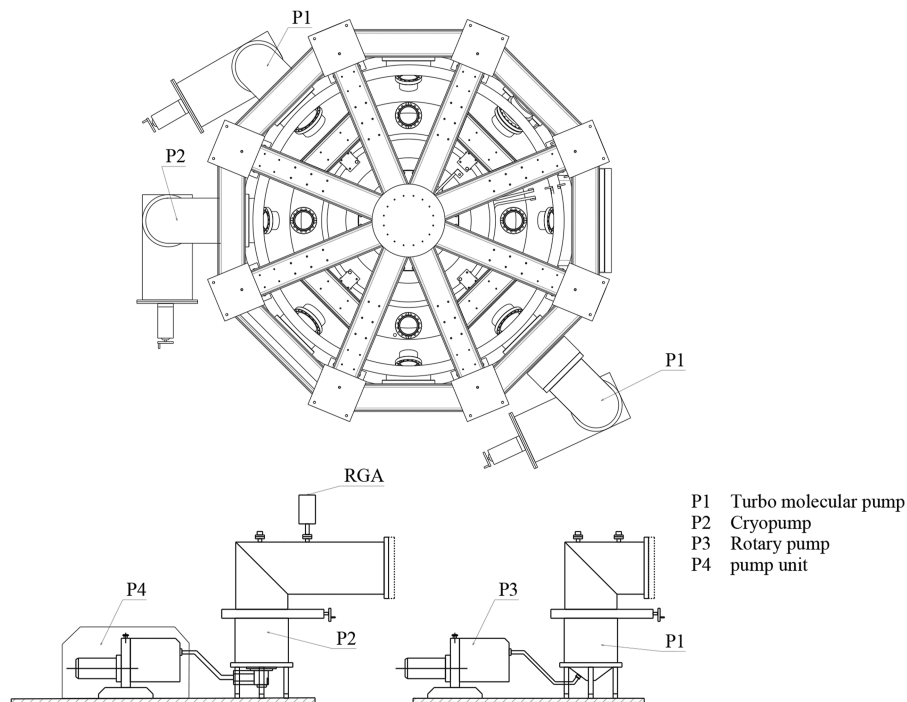


FIG. 2. Layout of the NCST pumping system.

TABLE I. Details of NCST vacuum equipment.

Label	Type	Number	Character	Function
SFJ-211	Helium mass-spectrometer leak detector	1	Minimum identify leaks 5×10^{-9} (Pa l/s)	Leak detection
ZDF-5227AX	Vacuum gauge	1	Measure range 1.0×10^{-5} to 1.0×10^5 (Pa)	Measure pressure of VV
ZDF-11A2	Vacuum gauge	1	Measure range 1.0×10^{-5} to 1.0×10^5 (Pa)	Measure pressure of VV
ZDR-12/0B6	Vacuum gauge	1	Measure range 1.0×10^{-8} to 1.0×10^{-1} (Pa)	Measure pressure of VV
SRS-RGA 100	Residual gas analyzers	1	Measure mass ranges of 1–100	Analyze the gas composition
WXG-16A	Rotary pump	2	Pumping speed 16 (l/s)	Fore pumps
CFB-2000Z	Turbo molecular pump	2	Pumping speed 2000 (l/s)	Main pumps
DZB250	Cryopump	1	Pumping speed (for water) 6900 (l/s)	Achieve ultimate vacuum

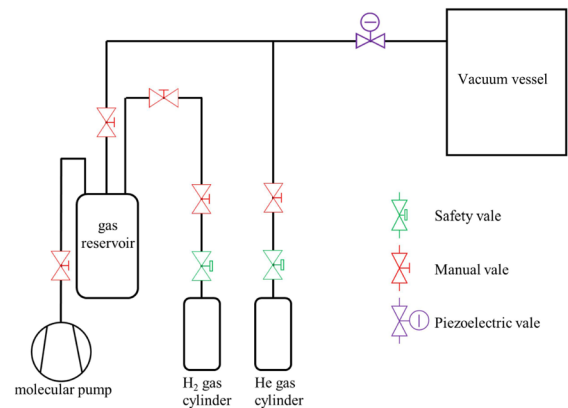
a pumping speed (for water) of 6900 l/s is installed on the horizontal port, and a pump unit is used as the roughing pump to assist the cryopump. More information on the vacuum pumps is provided in Table I.

The vacuum system of the NCST has three sets of vacuum gauges, and the specific measurement range is shown in Table I. In addition, a partial pressure measurement is performed by a quadrupole mass spectrometer probe residual gas analyzer (RGA). It is installed on the connecting duct of the cryopump. Leak detection is important for any vacuum system, and the NCST is equipped with a helium mass spectrometer, which can identify leaks of the order of 5×10^{-9} Pa l/s.

III. GAS PUFFING SYSTEM

The fueling system is an important part of the tokamak vacuum system. Gas puffing, supersonic molecular beam injection, and pellet injection are the most commonly used fueling methods. Among these, gas puffing is the most frequently used in tokamaks, and it is also used by the NCST. The gas puffing system includes a gas supply, transfer lines, a gas reservoir, pressure gauges, and piezoelectric valves, as shown in Fig. 3. At present, the working gas for the plasma discharge is hydrogen. Helium and hydrogen are the main working gases for glow discharge cleaning. In order to stabilize the hydrogen pressure, it is necessary to install a gas reservoir between the high-pressure gas cylinder and the puff nozzle.¹⁴ The volume of the reservoir is 25 l, and a pressure gauge is mounted on the reservoir. The pressure gauge ensures that the reservoir pressure is maintained at a fixed value. The main function of the reservoir is to maintain a consistent puff rate. At present, the pressure in the reservoir is set to 0.18 MPa.

The behavior of the working gas is generally considered an important factor in the overall performance of a tokamak. SUNIST experiments have shown that controlling the timing and amount of gas puffing is of great importance for the plasma discharge.¹⁵ The gas puffing time and gas amount are controlled by the PEV-1 piezoelectric valve in the NCST. The opening degree of the piezoelectric valve can be changed by the applied voltage, and the flow rate can then be adjusted accordingly. The piezoelectric valve has two modes: man-

**FIG. 3.** Schematic of the NCST gas puffing system.

ual control and automatic control. The manual control is only used for glow discharge cleaning on the VV.

IV. WALL CONDITIONING SYSTEM

The NCST wall conditioning process includes baking and discharge cleaning. Generally, the main baking methods are airflow baking and external heating. There are other heating methods, such as the baking of the VV by eddy currents used by KTX.¹⁶ In order to achieve successful plasma discharge, the ultimate vacuum pressure should reach 10^{-5} Pa before plasma operation.¹ However, it is difficult to achieve this target vacuum only through pumping. When the VV reaches a higher vacuum degree, the main factor affecting the vacuum degree is not the residual gas in the VV but the impurity particles released from the wall of the VV. The main components of the impurities are water and hydrocarbons. The VV outgassing rate is related to the wall gas content and temperature. Therefore, the wall of the VV and its internal components are baked to dissolve and desorb the impurities in the inner wall of the VV, thereby reducing the vacuum degree. As can be seen, baking plays an important role in improving vacuum quality. The baking of the NCST is carried out by an armored heating wire, and the maximum heating temperature is

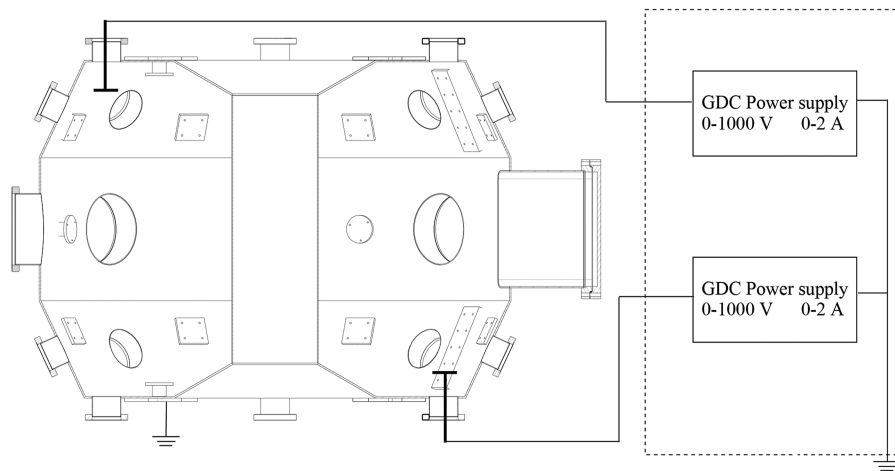


FIG. 4. Glow discharge cleaning (GDC) system.

set to 170 °C. The NCST baking process is divided into three stages: the heating stage, the isothermal stage, and the cooling stage. In the heating stage, the heating wire slowly increases the temperature by 5 °C/h. After heating to the set temperature, it enters the isothermal stage. After the isothermal stage is completed, the wall is cooled by a gradient of 5 °C/h, and the baking operation is completed when the temperature is reduced to about 30 °C.

Taylor discharge cleaning, glow discharge cleaning (GDC), and electron cyclotron resonance discharge cleaning have all been widely used for wall conditioning.¹⁷ GDC is selected for the conditioning of the first wall on the NCST and functions as follows: The GDC system uses a glow electrode as an anode and the inner wall of the device as a cathode. A certain voltage is then applied between the two poles, and an electric field is formed between the electrode and the inner wall. The ions in the VV plasma can continuously bombard the first wall surface after being accelerated by the electric field. In this process, ions transfer their energy to impurity gas molecules or atoms on the surface. Then disrupt their binding to the wall surface molecules or react with them to form gaseous compounds, causing them to desorb from the wall and be extracted from the VV.

The NCST is equipped with two anodes, each comprising a disk and a stainless steel rod. The thickness of the disk is 5 mm, and the

diameter is 80 mm. The two anodes are installed at the bottom and top of the VV. As shown in Fig. 4, the GDC power supply system can provide currents of 0–2 A and voltages of 0–1000 V. A typical image of the discharge cleaning is shown in Fig. 5, and the specific parameters are as follows: For helium, the GDC pressure is set to 1×10^{-2} – 5×10^{-2} Pa, the anode voltage is set to 500 V, and the current is set to 1 A; for hydrogen, the GDC pressure is set to 1–9 Pa, the anode voltage is set to 500 V, and the current is set to 1 A.

V. EXPERIMENTAL RESULTS

A high-quality vacuum environment is an essential prerequisite for the NCST to realize successful plasma discharge. The experimental results for pumping and baking are presented in this section. The vacuum pressure and baking temperature curves are shown in Fig. 6. The rotary pump serves as the roughing pump and is started first. Once the VV pressure drops below 10 Pa, the molecular pump is

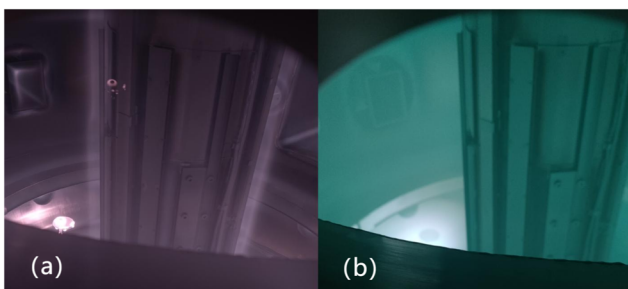


FIG. 5. Snapshots of the GDC using different working gases (a): pure hydrogen gas, (b): pure helium gas.

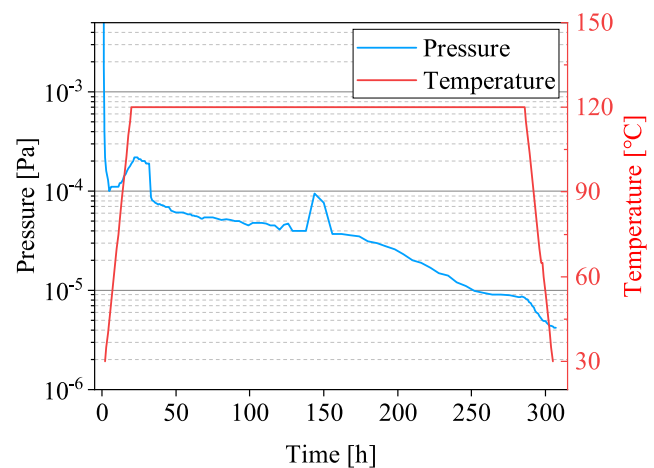


FIG. 6. Pumping curves and baking temperature in the NCST.

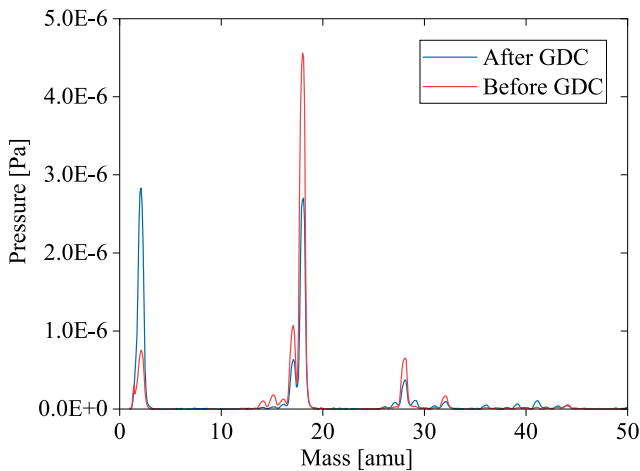


FIG. 7. Partial pressure in the VV before and after GDC.

activated. As shown in Fig. 6, the pressure of the VV dropped rapidly after the molecular pump was started, and the baking was turned on when the pressure dropped to 2.2×10^{-4} Pa. As mentioned earlier, the baking temperature should be raised slowly and evenly to avoid leakage due to uneven heating. It took 18 h for the temperature to rise from 30 to 120 °C (an increase of 5 °C/h). The vacuum pressure dropped rapidly at 32 h because the cryopump was started at that time. There was a small spike between 144 and 156 h, because the cryopump valve was closed. The 12 h 144–156 were used for cryopump regeneration. At 286 h, the vacuum was further reduced by turning off the baking process. Finally, an ultimate pressure of 4.2×10^{-6} Pa was achieved after 307 h of pumping, which meets the discharge requirements.

After baking, the impurities in the VV wall were greatly reduced, but in order to further improve the vacuum environment, it was necessary to perform GDC. The typical mass spectra of the residual gases in the VV before and after one night of GDC are shown in Fig. 7. It can be seen that the percentage of water



FIG. 8. Plasma discharge images for different vacuum environments: (a) Shot No. 210523021: the vacuum environment is bad; and (b) Shot No. 220914026: the vacuum environment is good.

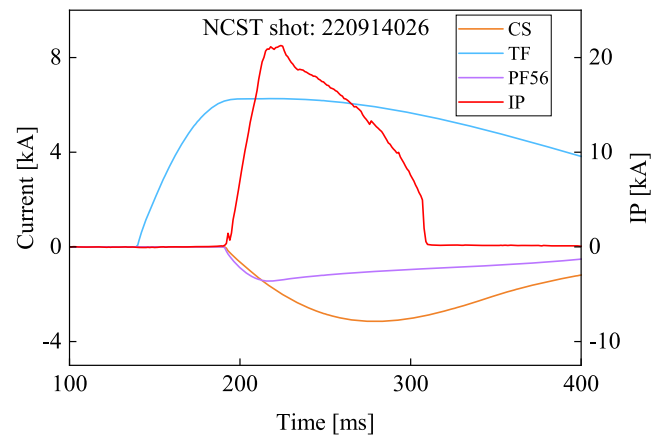


FIG. 9. Coils and plasma currents for the NCST plasma discharge.

decreased from 68.4% to 45%. Generally, hydrogen GDC is followed by helium GDC. Hydrogen GDC is used to remove oxygen impurities, while helium GDC removes residual hydrogen from the wall of the VV. After the wall conditioning was completed, the plasma discharge experiments were started to test the whole vacuum system. Figure 8 shows pictures taken by a high-speed camera during plasma discharge in different vacuum environments. When the vacuum environment was poor, the light emitted was blue, as shown in Fig. 8(a). Clear dust can be observed in the figure, indicating that the vacuum environment and wall conditions failed to meet the discharge requirements. In contrast, in a good vacuum environment, the light emitted was red in Fig. 8(b), indicating that it was mainly H α radiation and no impurities were seen. A good vacuum environment is the premise of successful plasma discharge, so successful plasma discharge also proves that the vacuum environment is good. In the 220914026 shot, a discharge with a plasma current of more than 21 kA and a duration of 100 ms was obtained, which validates the NCST vacuum environment. The NCST VV total leakage and outgassing rate for 12 h was 1.50×10^{-4} Pa l/s, as measured by closing the gate valve after ending the plasma discharge experiment. The temporal profiles of the coil current and plasma current are shown in Fig. 9. The experimental results demonstrate that the NCST vacuum system is effective and steadily improves vacuum quality.

VI. SUMMARY

The NCST is a new spherical tokamak currently located at Nanchang University in China. It can serve as an educational device for performing experiments to cultivate fusion for specialized graduate students.

The NCST vacuum system consists of three main parts: a pumping system, a gas puffing system, and a wall conditioning system. The experimental results in this paper indicate that the pumping system can easily pump the VV pressure to 4.2×10^{-6} Pa. The gas puffing system can accurately seed gas to meet the plasma discharge and GDC gas requirements. In the wall conditioning component, baking and GDC can effectively remove water and other impurities from the VV wall, which further promotes the quality of the vacuum environment. Under high-quality vacuum conditions,

discharges with a plasma current of more than 21 kA and a duration of 100 ms were obtained. It can be inferred that the vacuum system is reliable and can meet the daily experimental requirements of the NCST.

At present, the NCST vacuum system is being upgraded, and an SMBI system will be installed in the NCST. SMBI has several advantages compared with conventional gas puffing, such as a larger penetration depth and a higher fuel efficiency.^{18–20}

ACKNOWLEDGMENTS

This work was supported by the National Key Research and Development Program of China (Grant No. 2022YFE03070002), the Project of Scientific and Technological Innovation Base of Jiangxi Province (Grant No. 20203CCD46008), the Natural Science Foundation of Jiangxi Province (Grant No. 20212BAB211025), and the Jiangxi Province Key Laboratory of Fusion and Information Control (Grant No. 20171BCD40005).

AUTHOR DECLARATIONS

Conflict of Interest

We declare that we have no financial or personal relationships with other people or organizations that can inappropriately influence our work, and there is no professional or other personal interest of any nature or kind in any product, service, or company that could be construed as influencing the position presented in this or revised version of the article.

Author Contributions

Fu Hua Huang: Data curation (equal); Writing – original draft (lead). **Dong Hua Xiao:** Data curation (equal). **Xiao Chang Chen:**

Writing – review & editing (equal). **Hui Chen:** Writing – review & editing (equal). **San Qiu Liu:** Writing – review & editing (equal).

DATA AVAILABILITY

The data that support the findings of this study are available from the corresponding authors upon reasonable request.

REFERENCES

- ¹J. S. Hu, Z. Cao, G. Z. Zuo *et al.*, *Fusion Eng. Des.* **177**, 113058 (2022).
- ²Z. Khan, F. Pathan, S. George *et al.*, *Fusion Eng. Des.* **88**, 692 (2013).
- ³S. H. Seo, H. T. Kim, K. P. Kim *et al.*, *Rev. Sci. Instrum.* **79**, 116103 (2008).
- ⁴H. Ran, B. Song, J. Hou *et al.*, *Fusion Sci. Technol.* **77**, 549 (2021).
- ⁵Z. Cao, C. H. Cui, D. Q. Liu *et al.*, *Plasma Sci. Technol.* **7**, 2632 (2005).
- ⁶L. H. Yao, J. F. Dong, Y. Zhou *et al.*, *Nucl. Fusion* **44**, 420 (2004).
- ⁷M. Shimada and R. A. Pitts, *J. Nucl. Mater.* **415**, S1013 (2011).
- ⁸Y. C. Huang, H. Ran, L. J. Cai *et al.*, *Fusion Eng. Des.* **158**, 111847 (2020).
- ⁹M. Hou, Y. Z. Qian, S. Q. Liu *et al.*, *AIP Adv.* **12**, 025106 (2022).
- ¹⁰T. B. Ouyang, Y. Z. Qian, S. Q. Liu *et al.*, *AIP Adv.* **12**, 015314 (2022).
- ¹¹T. B. Ouyang, H. Chen, S. Q. Liu *et al.*, *Rev. Sci. Instrum.* **94**, 013509 (2023).
- ¹²A. Mancini, J. Ayllon-Guerola, S. J. Doyle *et al.*, *Fusion Eng. Des.* **171**, 112542 (2021).
- ¹³Y. T. Song, S. T. Wu, J. G. Li *et al.*, *IEEE Trans. Plasma Sci.* **42**, 503 (2014).
- ¹⁴X. W. Zheng, J. G. Li, J. S. Hu *et al.*, *Plasma Phys. Control. Fusion* **55**, 115010 (2013).
- ¹⁵H. Q. Xie, Y. Tan, R. Ke *et al.*, *Plasma Sci. Technol.* **16**, 732 (2014).
- ¹⁶W. D. Liu, T. Lan, W. Z. Mao *et al.*, *Nucl. Fusion* **57**, 116038 (2017).
- ¹⁷Y. H. Ding, G. Zhuang, W. J. Wang *et al.*, *Plasma Devices Oper.* **17**, 207 (2009).
- ¹⁸D. L. Yu, C. Y. Chen, L. H. Yao *et al.*, *Nucl. Fusion* **50**, 035009 (2010).
- ¹⁹X. L. Yuan, J. G. Li, J. H. Wu *et al.*, *Fusion Eng. Des.* **134**, 62 (2018).
- ²⁰H. Takenaga, Y. Miyo, J. Bucalossi *et al.*, *Nucl. Fusion* **50**, 115003 (2010).